Low-Energy Gamma Radiation in the Atmosphere at Midlatitudes

R. C. HAYMES, S. W. GLENN,[1] G. J. FISHMAN, AND F. R. HARNDEN, JR.

Department of Space Science
Rice University, Houston, Texas 77001

Balloon-borne experiments with directional scintillators that measured the spectrum of gamma radiation with energies between 30 and 570 kev in the atmosphere up to 130,000 feet were conducted during 1967 and 1968. These data are of interest in connection with understanding the origin of atmospheric photons and with estimating planetary and stellar gamma albedos, as well as effecting improvements in gamma-ray astronomy. The measurements, conducted in the United States and in Australia, showed that a continuum and structure are present at depths X greater than 90 g cm^{-2}; the intensity of the continuum depends exponentially on depth for $X \geq 102$ g cm^{-2}, but the shape is relatively depth-independent. The spectrum softens considerably at lesser depths. Structure is observed in the spectrum at 130,000 feet, superimposed on a continuum approximated by the power law $27.8E^{-1.87}$ photons cm^{-2} sec^{-1} ster^{-1} kev^{-1}. The latitude, altitude, and energy variations of the spectrum are discussed in terms of the various factors responsible at various depths for the spectrum; it is shown that several factors are responsible for the continuum and that the observed structure is mainly due to (n, γ) effects from cosmic-ray neutrons, and an upper limit is established for a line flux at 511 kev. The 95% confidence level upper limit of 0.2 photon cm^{-2} sec^{-1} for line radiation at the positron annihilation energy is slightly below the fluxes previously reported by others.

1. INTRODUCTION

This paper reports upon some measurements of the energy spectrum of atmospheric gamma-ray photons that have energies between 30 and 570 kev, an interval that extends from the X ray to beyond the positron annihilation energy at 511 kev and that includes many of the energies of nuclear transitions associated with the various radioactive species. The data were acquired from near sea level to balloon altitudes of ~130,000 feet, at midlatitudes during 1967 and 1968.

Some of the features of low-energy atmospheric gamma radiation have been explored previously [*Perlow and Kissinger*, 1951; *Anderson*, 1961; *Jones*, 1961; *Vette*, 1962; *Peterson*, 1963; *Chupp et al.*, 1967; *Womack and Overbeck*, 1968]. No spectra of the radiation deep within the atmosphere have been published, but an exponential dependence of the intensity on atmospheric depth has been found there. The gamma-ray flux reaches a maximum value at

~100 g cm^{-2}, although the precise value may be latitude-dependent. At high altitudes, a very steep atmospheric spectrum with a line at 511 kev was first reported by *Peterson* [1963]; later work has indicated that annihilation radiation originates predominantly in the mass surrounding the detector [*Womack and Overbeck*, 1968].

Various possibilities have been discussed as sources of low-energy gamma photons in the atmosphere at mid- and low-latitudes. The altitude variation of the spectrum has implications for our understanding of the origin of these photons. Included in this list of candidate source mechanisms are: (*a*) the low-energy end of the cosmic-ray electromagnetic component; (*b*) photons originating from the nucleonic component of the cosmic radiation; (*c*) positron annihilation in the atmosphere; (*d*) fission products from tests of nuclear and thermonuclear devices; (*e*) Compton scattering of high-energy photons arising from the above processes; and (*f*) the diffuse radiation from the cosmos. Measurements made with moderately high-energy resolution of the dependence of spectral shape on altitude may help establish

---

[1] Present address: McDonnell Automation Co., Houston, Texas 77058.

the relative importance at various depths of these factors through a comparison of the gamma-ray data with those of the candidates listed above. Each of the planets and the sun will be a source of gamma radiation because of photon leakage from their atmospheres; a gamma-ray albedo will be present around each such celestial object, and high-altitude studies conducted within the earth's atmosphere may be helpful in estimating the magnitude of the albedo. The diffuse radiation observed at a given altitude represents a background for astronomical investigations of discrete sources; an understanding of this background may permit an improvement in astronomical experiments.

2. APPARATUS

The balloon-borne detector is a two-inch thick NaI(Tl) crystal, four inches in diameter. Gamma radiation incident upon this detector is collimated by an outer crystal; active collimation is employed that rejects charged radiation as well as collimates the incident photons. (The active collimation also serves to suppress Compton photons.)

Charged-particle rejection is also provided by a thin (¼″ thick) plastic scintillator that covers the aperture of the central detector. Like the photomultipliers viewing the outer crystal, the tubes viewing the plastic disk are connected in anticoincidence with the phototube attached to the central detector. Hence, 4π rejection is accomplished.

The geometrical half-flux angle is about 9° from the axis; measurements show that this is actually the case for a remote point source at X-ray energies, since a nearly triangular angular-response function with this half-angle is observed in the laboratory at low energies. The collimator, however, is only about 2 mean free paths thick on the sides at 500 kev; some leakage through the shield does occur at these higher energies. One result of the leakage is that the point-source response function is broadened at increased energies; 12° is the half-flux angle at 511 kev. If the instrument is immersed in isotropic radiation, the leakage flux dominates the counting rate at energies in excess of 350 kev.

An energy resolution of 10%, FWHM, was measured for one instrument at $E = 511$ kev.

The resolution of the other detector was 13%, FWHM; both resolution measurements were made with the full complement of flight electronics shortly before and after each flight. The pulse height versus energy calibration was measured to ±4 kev. The system was kept at a temperature of 80° ± 1° by thermostatically controlled heaters and by insulation, on each of the balloon flights described herein, so that the gain of the system would remain constant. No spectral changes at a constant altitude larger than ±1 pulse-height analyzer channel (out of 128) were detected during any of the flights.

The central photomultiplier, mounting hardware, and thin plastic sheet attenuate the photon flux reaching the central crystal. Corrections must be made for these effects, as well as for the intrinsic photopeak detection efficiency calculated by *Miller et al.* [1957], and tested by *Neiler and Bell* [1965] and for the escape of K-shell X-radiation from the central crystal as determined by *Axel* [1954]. Figure 1 shows the various corrections as a function of photon energy. The corrections due to phototube and plastic-scintillator absorption were experimentally determined in our laboratory with radioactive sources; the counting rate of the central detector was compared with that of a similar unshielded 4″ × 2″ NaI(Tl) crystal, exposed to the same flux.

The directional instrument automatically tracks celestial sources in their diurnal motion with a balloon-borne equatorial drive system. The polar axis is oriented parallel to the earth's rotational axis by an azimuth servosystem that locks onto the geomagnetic field; compensation for the average declination of the field over the expected trajectory is applied to each flight. The polar axis is automatically rotated 180° in azimuth every 10.5 minutes during each flight so that the background may be measured; it is these background data that are discussed in this paper.

Some of the balloon flights discussed herein also carried aloft an ionization chamber of the type described by *Neher* [1953], and by *Neher and Johnston* [1956]. This instrument was kindly loaned to us by Prof. H. V. Neher and was added to the airborne apparatus in order to monitor the intensity of the ionizing radiation. As discussed by *Anderson et al.* [1967], such
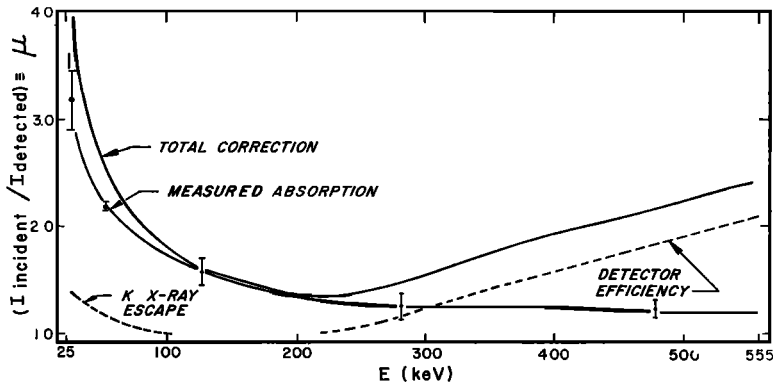
Fig. 1. Plot of the total correction factor μ versus photon energy E. The attenuation points were measured in the laboratory; the other curves were calculated from the work of others, as discussed in the text.

chambers are sensitive to photons with energies in excess of 30 kev, but respond primarily to charged particles, such as protons with energies greater than 10 Mev.

The telemetry subsystem devoted 40 time-shared channels to engineering data. The 5-kilobits/sec data rate resulted in only minor telemetry losses.

Pressure altitudes were measured with a Metrophysics Corporation transducer, the output of which depends on the thermal conductivity of the local atmosphere. Since the transducer was located over 100 feet below the base of the balloon on each flight, it is believed that the calibration was unaffected by any outgassing of helium; the pressures appear to be accurate to ±0.1 mb. This pressure measurement was compared in the data analysis with the readings of a telemetered aneroid 'beacon' and a separate photographically recorded aneroid 'photobarograph.' It frequently but not always indicated pressures near the mean of those recorded by the two aneroids; the discrepancies, however, never exceeded 1 mb.

3. FLIGHTS

We discuss here the results from five flights; each measured radiation from ~30 kev to an upper electronically imposed limit that varied from flight to flight between 555 and 570 kev. Three of the balloons were launched in 1967 from Palestine, Texas, in the United States. The other two flights were conducted in 1968 from Mildura, Victoria, Australia. Since the two sites are approximately equidistant from

the geographic equator, it is of interest to compare the radiation in the atmosphere above those locations.

The first Palestine flight took place on June 4, 1967; the other two occurred on August 10 and 29, 1967, respectively, whereas the Australian launches occurred on April 23 and May 6, 1968. All five thus took place during a time short compared with the solar cycle. The Environmental Science Services Administration reports [ESSA, 1967; 1968] show that the largest solar events observed during any of the flights were normal subflares. The planetary magnetic index, Kp, was also low during the measurements.

All of the flights reached the same pressure-altitude, nominally 3 g cm⁻², or about 130,000 feet. The ascent rates varied considerably, permitting detailed exploration of the radiation at various intermediate atmospheric depths.

4. RESULTS

Counting rates as a function of time and pulse height represent the gamma-ray raw data. Raw data obtained on August 29, 1967, over Texas at ~3 g cm⁻² atmospheric depth are shown in Figure 3. In all of the data discussed here, the detector was aimed away from known discrete sources of hard radiation, so that the 'background' for astronomical investigations could be measured.

In order that meaningful interpretations and comparisons with other work may be made, the observed counting rates must be converted to a flux, in absolute units. Such a conversion is not

possible with only the data available from this experiment; some assumptions must be made in addition.

Thus, we have assumed that the energy spectrum outside the energy interval measured in these experiments decreases at least as steeply as that observed. We have also assumed that multiple Compton scattering is negligible in a detector of the dimensions indicated for the energy interval of interest. Assumptions must also be made regarding the angular distribution of the incident radiation. We have assumed it to be isotropic at atmospheric depths greater than one mean free path from the top of the atmosphere and at altitudes sufficiently high that gamma radiation from the planetary surface is absorbed. As will be seen in the next section, this assumption of isotropy is not grossly invalid even at the highest altitudes considered in the present work.

A quantity required for the conversion is the 'effective solid angle,' $S(E)$. It is the solid angle subtended by the central crystal and is defined by

$$S(E) = 2\pi \int_0^{\pi} e^{-x\tau} \sin \theta \, d\theta \qquad [\text{ster}] \qquad (1)$$

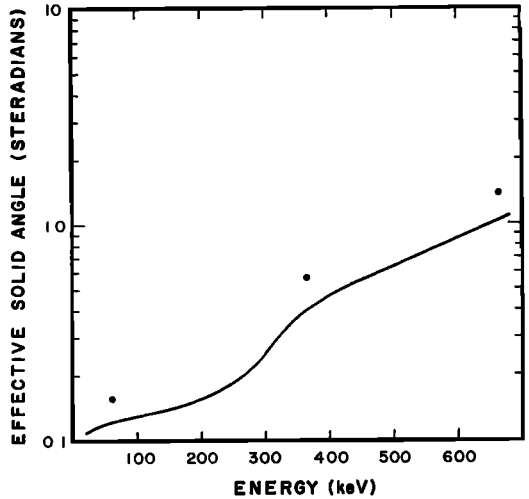for cylindrical symmetry. In equation 1, $x = x(\theta)$ is the path length through the collimator

Fig. 2. Effective solid angle as a function of energy. The points were measured in the laboratory with radioactive sources; the curve was calculated using equation 1. It is seen that there is satisfactory agreement between the points and the shape of the curve, but there is ~20% discrepancy in the absolute values.

as a function of angle θ from the axis. $\tau(E)$ is the absorption coefficient at photon energy E.

Figure 2 shows the results of the calculation of S. The solid curve in the figure is the calcu-
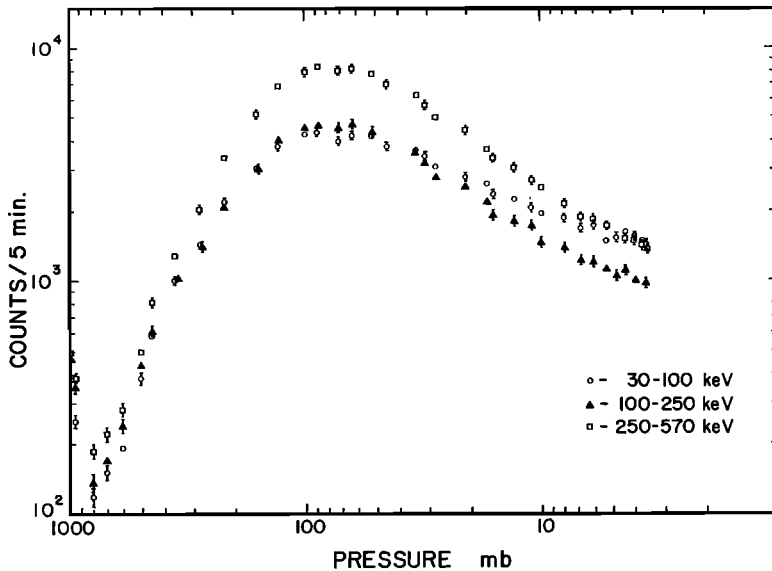

Fig. 3. Flux (in three energy groups) measured as a function of atmospheric depth over Texas on August 29, 1967.
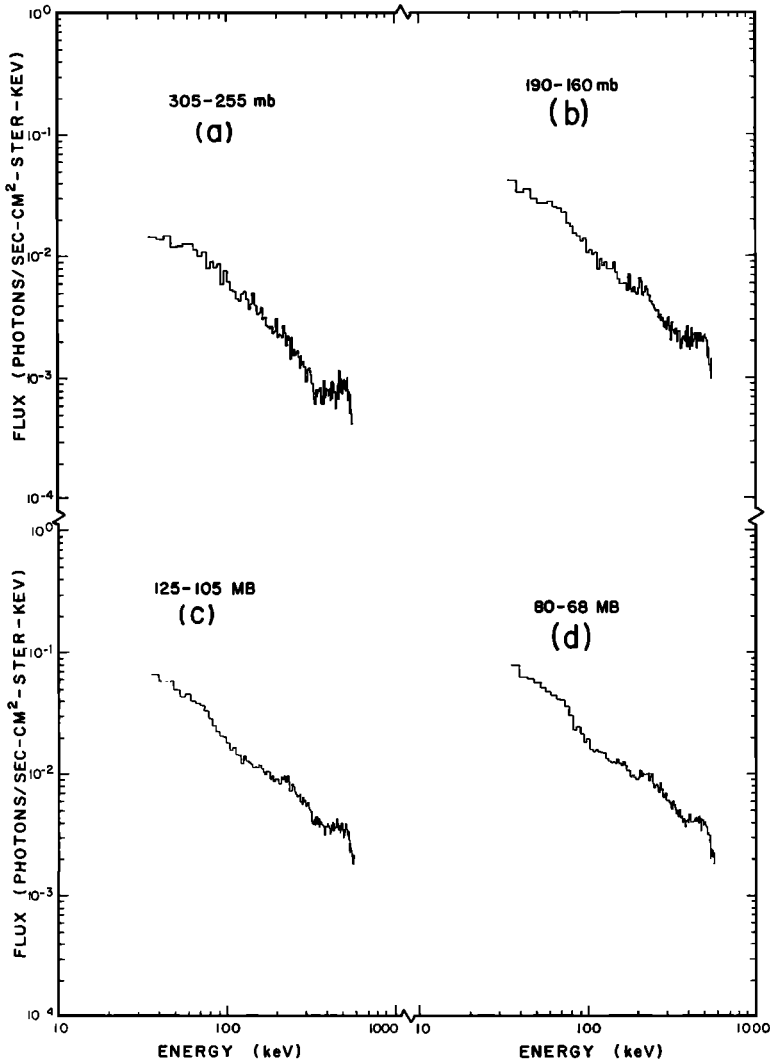
Fig. 4. Low-altitude fluxes measured on August 29, 1967, over Texas. The various depth intervals are shown; errors are discussed in the text.

lated result. The three points were measured with radioactive sources. There is satisfactory agreement with the shape of the curve. The assumptions are presumably responsible for the ~20% discrepancy in the absolute values. We have normalized the curve to the 3 measured points for the calculations described below.

If $C(E)$ is the observed counting rate in a given pulse-height channel, $S(E)$ may be used to convert from $C(E)$ to the flux $F(E)$, through the relationship

$$F(E) = \frac{C(E)\mu(E)}{A\,W\,S(E)}\left[\frac{\text{photons}}{\text{cm}^2\,\text{sec ster kev}}\right] \quad (2)$$

where $\mu(E)$, which is shown in Figure 1, is the product of the correction factors for photopeak efficiency, K X-ray escape, and instrumental absorption. In equation 2, A is the area of the front surface of the central crystal; W is the width of a pulse height analyzer channel, in kev. Thus $F(E)$ represents the differential flux at an energy E.

Figures 3–7 show the August 29, 1967, results obtained at atmospheric pressures from 280 to 3.5 mb, over Texas. (This corresponds to an altitude range of approximately 8 to 40 km.) The discrepancies observed in the laboratory lead us to assign about a ±20% absolute error to the fluxes shown in the figures.

The data have been summed into only three energy intervals in Figure 3 for clarity. The summation also serves to improve the statistics.

For comparison purposes, we have also shown in Figure 7 the spectral results obtained by other investigators at various altitudes near the top of the atmosphere and at various latitudes.

The power law that best fits the continuum portion of the (Figure 7) high-altitude spectrum is given by $F(E) = 27.8E^{-1.67}$ photons cm^{-2} sec^{-1} ster^{-1} kev^{-1} at energies between 35 and 160 kev; it appears reasonable that the higher-energy continuum is but an extension of that spectrum.

Data were also obtained, on the 1967 flights, from the ionization chamber. Figure 8 shows the data obtained on August 10 with that instrument. It also shows, for comparison purposes, data taken by *Anderson* [1961] with a similar instrument at a similar geomagnetic latitude, approximately nine years earlier.
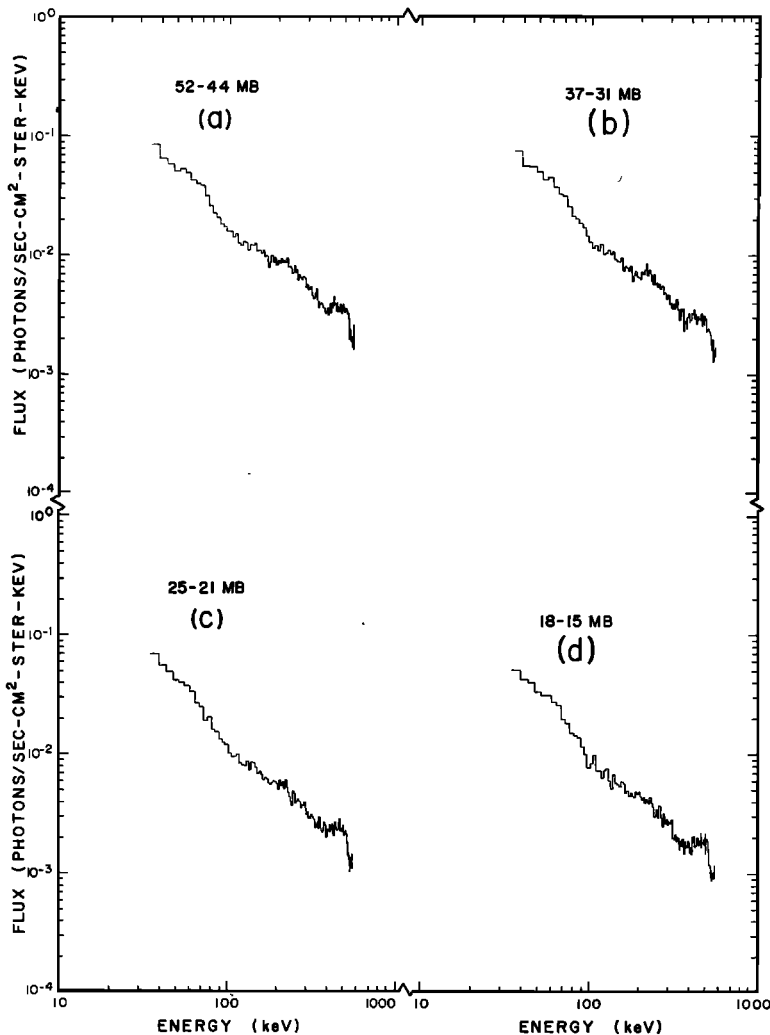

Fig. 5. Middle-altitude fluxes measured on August 29, 1967, over Texas. The various depth intervals are shown; errors are discussed in the text.
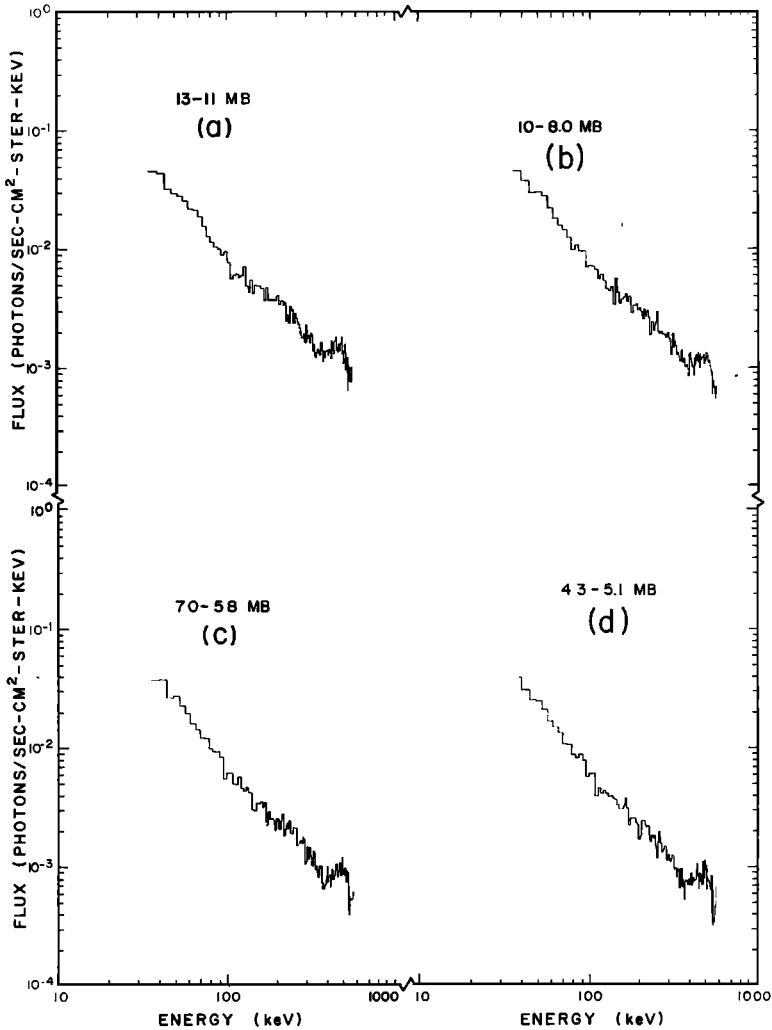
Fig 6. High-altitude fluxes measured on August 29, 1967, over Texas. The various depth
intervals are shown; errors are discussed in the text.

5. DISCUSSION

Figure 3 illustrates the dependence on depth for three representative energy groups. As the detector leaves the planetary surface, a significant drop occurs in the intensity of the gamma radiation; the radioisotopes in the earth are progressively further away, so that the flux from the earth decreases. The particular radioisotopes in the local terrain determine the spectral shape near the planet's surface; elements such as radium produce lines at energies in excess of 1 Mev.

After the detector reaches altitudes greater than a few thousand feet, an increase with increasing altitude is observed to commence. This increase is characteristic of the behavior of the secondary cosmic radiation below the transition maximum within the earth's atmosphere.

An exponential of the form

$$F(p, E) = A(E) + B(E)e^{-p/D(E)} \qquad (3)$$

may be fit to the data at pressures p such that $710 \text{ mb} \geq p \geq 102 \text{ mb}$. In (3), $F(p, E)$ is the flux in units of 10^{-4} photons/cm² sec ster kev, and A, B, and D are energy-dependent num-

bers; $D(E)$ may be interpreted as the mean free path for absorption in millibars ($\sim$g cm^{-2}), and A and B indicate the relative intensity of the radiation at the various energies E considered. Table 1 shows the results of the fit.

Figure 9 illustrates the dependence on energy. Most of the data points shown in Figure 9 indicate that the absorption length of the gamma radiation is closer to the 123 g cm^{-2} associated with the soft component of the cosmic radiation [*Puppi and Dallaporta*, 1952] than with the fast neutron absorption length of 169 g cm^{-2} [*Haymes*, 1964]. We, therefore, conclude that

the low-altitude gamma radiation is most likely a product of the electromagnetic component of the cosmic radiation, rather than the nucleonic component.

There are additional data available that support this conclusion. The measured depth of the maximum, 58–92 g cm^{-2} (corresponding to an altitude of 55,000–65,000 feet), is the same for all photon energies considered here and agrees with that found by *Brini et al.* [1967] at a slightly higher latitude. A comparison of Figures 3 and 8 indicates that the gamma ray maximum and the ionizing-radiation maxi-
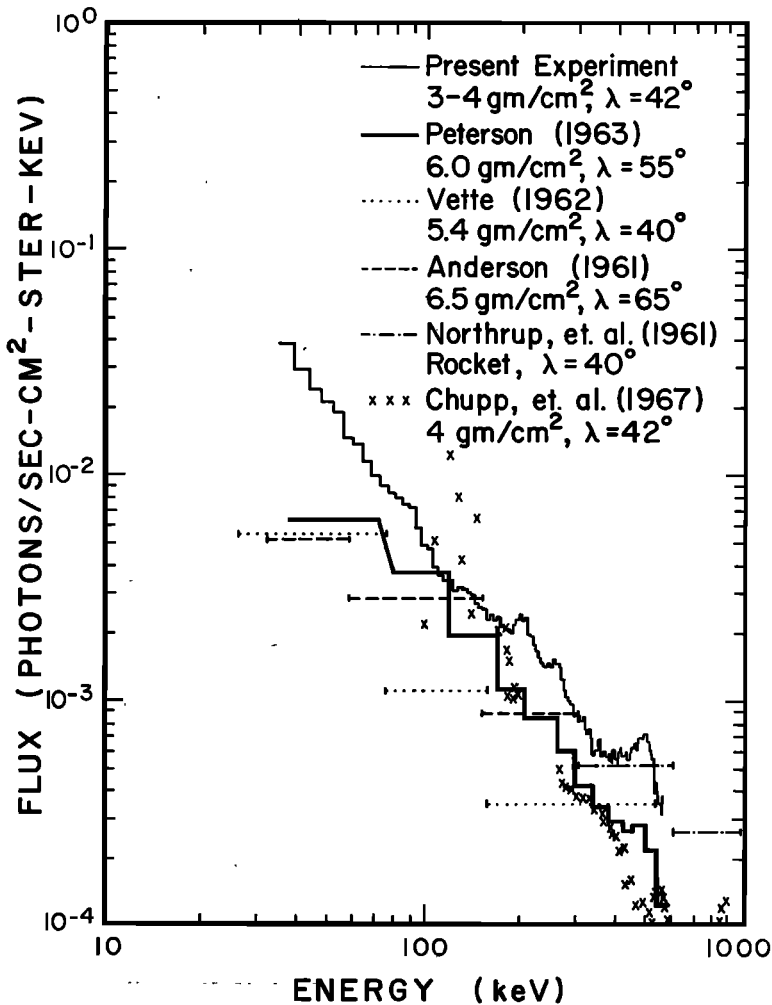

Fig. 7. Gamma-ray spectrum measured at 3–4 g cm^{-2} over Texas on August 29, 1967; the errors are discussed in the text. Also shown are the earlier results obtained by others at several depths near the top of the atmosphere at various latitudes, with differing instrumentation. No corrections for efficiency, etc., have been applied to the earlier results.
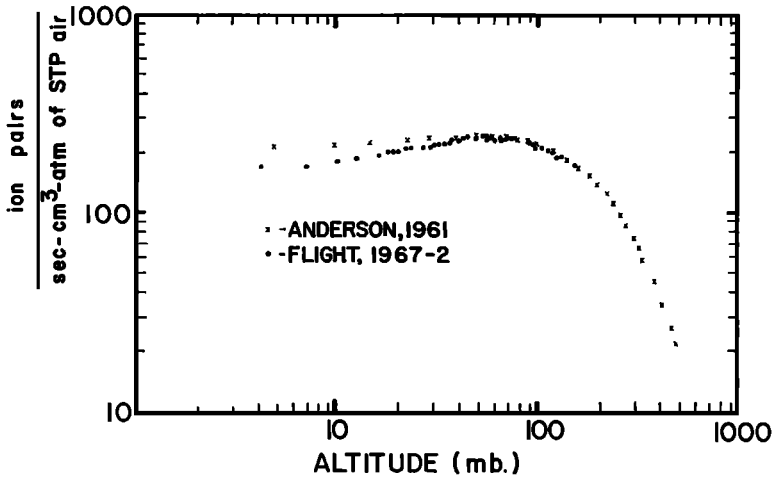
Fig. 8. Ionization chamber data as a function of atmospheric depth over Texas on August 10, 1967. The 1958 results of Anderson at comparable latitudes are shown for comparison purposes.

mum lie within 300–13,000 feet or 8–42 g cm⁻³ of each other, with the gamma-ray maximum occurring at somewhat lesser altitudes than the maximum recorded by the ion chamber.

Gamma spectra taken within the earth's atmosphere at a given latitude and depth may vary considerably in time. The variability may change the measured values of A, B, and D. A comparison of the fluxes shown in Figures 3 and 10 provides an illustration of the variability encountered well within the atmosphere.

The artificial deposition of radioactive substances in the atmosphere may be one source of such a temporal variation. Another possible source of spectral time-variability is solar activity. We have obtained some preliminary evidence that even events as small as subflares may generate sufficient hard radiation to be detectable at high balloon altitudes, but many more data must be obtained on solar outbursts at these energies before any conclusions on them may be drawn.

It is of interest to inquire into the dependence of spectral shape on altitude. Spectral shape may be described in terms of 'color indices.' Three such indices, α, β, and δ, are defined as follows:

$\alpha \equiv$ (flux between 30 and 100 kev)/(flux between 250 and 560 kev).

$\beta \equiv$ (flux between 100 and 250 kev)/(flux between 250 and 560 kev).

$\delta \equiv$ (flux between 30 and 100 kev)/(flux between 100 and 250 kev).

These three color indices are plotted versus the atmospheric pressure in Figure 11 for pressures less than ~800 mb on the August 29, 1967, flight. It is seen that the shape is roughly independent of altitude at pressures between ~90 mb and ~800 mb, but softens dramatically at lesser pressures; the rate of decrease of counting rate with increasing altitude is much less at $p < 90$ mb for the low-energy radiation than it is for high-energy photons. The spectral

TABLE 1. Results of Fitting the Equation
$F(p, E) = A(E) + B(E) \exp - p/D(E)$ at 710 mb $\geq p \geq$ 102 mb

Energy Interval, kev	$A(E)$*	$B(E)$*	$D(E)$*
30–100	5.1 × 10⁻⁴	782.8 × 10⁻⁴	139.1
100–250	3.1 × 10⁻⁴	221.6 × 10⁻⁴	140.3
250–560	0.96 × 10⁻⁴	101.6 × 10⁻⁴	113.2

* Units of A and B are photons cm⁻² sec⁻¹ ster⁻¹ kev⁻¹; D is expressed in millibars.

softening in the atmosphere sets in just above the altitude of maximum flux.

Several possibilities suggest themselves as responsible for the apparent change in spectrum. One such possibility is that the radiation may be anisotropic at great altitudes. Near the top of the atmosphere most of the radiation is produced in the lower hemisphere; the majority of the photon flux might perhaps be expected to be outward-directed, except for the cosmic component.

Brini et al. [1967] have experimentally verified isotropy at depths greater than 10 g cm⁻², by flying upward- and downward-aimed detectors. At yet higher balloon altitudes, *Frost et al.* [1966] observed that the flux of upward-moving photons at energies below 300 kev was about 30% greater than the downward-directed flux; the anisotropy was less at other energies.

Another factor that will influence the spectrum measured at a given atmospheric depth is the diffuse radiation from the cosmos. This was first measured by *Metzger et al.* [1964] with the Ranger 3 and 5 cislunar spacecraft. *Fazio* [1967] has summarized the data then available on this radiation; the differential number spectrum may be approximated in the energy range of interest by $30E^{-2}$ photons cm⁻² sec⁻¹ ster⁻¹ kev⁻¹. The steep E^{-2} dependence implies that this radiation will only be important
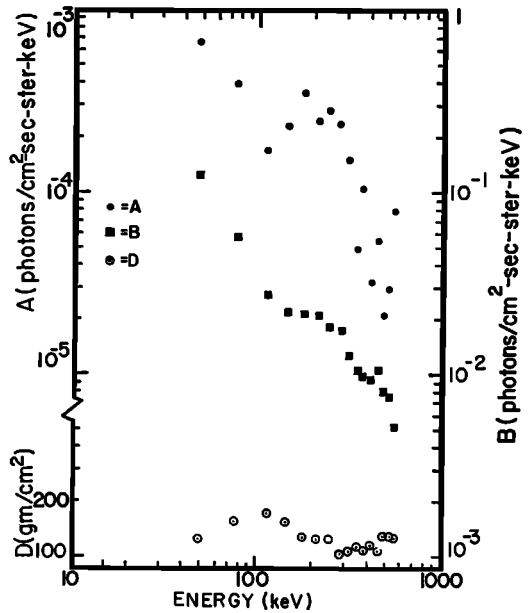

Fig. 9. Energy dependence of the parameters A, B, and D, introduced in equation 3.

at small depths; atmospheric absorption will rapidly eliminate it. The detector is rotated about the polar axis at the sidereal rate in our experiments. The hour angle at the time that the balloon halts its ascent and begins floating is such that the zenith angle is often but not
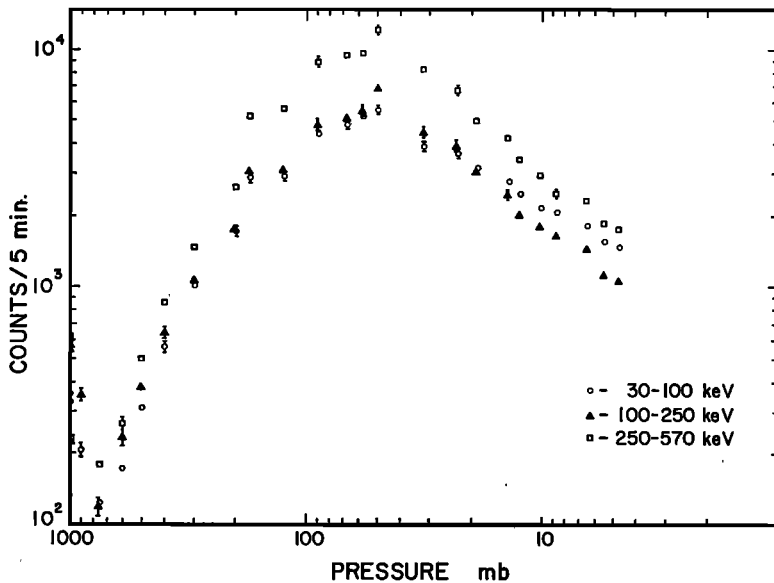

Fig. 10. Flux as a function of atmospheric depth over Texas measured on August 10, 1967.
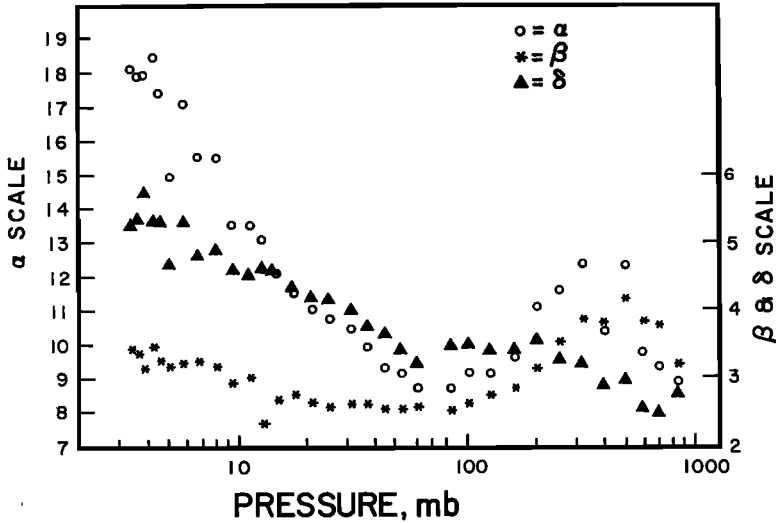
Fig. 11. Variation of color indices with atmospheric depth on August 29, 1967. A pronounced softening of the spectrum is observed at pressures less than 90 mb.

always ~45°, and absorption by the air of the cosmic component has mostly been near-complete on the ascent portions of the flights discussed here.

Using a flat-earth approximation, the ratio of the intensity of the celestial component to the total intensity may be estimated at a given atmospheric depth, for various zenith angles. The result for 3.9 mb is shown in Figure 12. The complex shape of the observed spectrum at high altitudes is responsible for the general shape of the curves in the figure. The fraction of the flux integrated over all energies is given in Figure 13. It is seen that the cosmic flux is less than ~25% of the total, at the zenith at typical balloon altitudes. The cosmic contribution reaches a maximum at ~100 kev at the zenith at 4 g cm^{-2}, where it is about $\frac{1}{3}$ of the flux observed at 41°N geomagnetic latitude. The steep nature of the cosmic spectrum thus does soften the total energy distribution, but it does not appear to be sufficiently intense to account for all of the observed softening of the midlatitude spectrum.

It may be a more significant fraction of the total at latitudes closer to the geomagnetic equator, since the cosmic flux is latitude independent [Bleeker et al., 1968]. Figure 14 shows the variation in flux encountered on one 1967 flight that increased its geomagnetic latitude
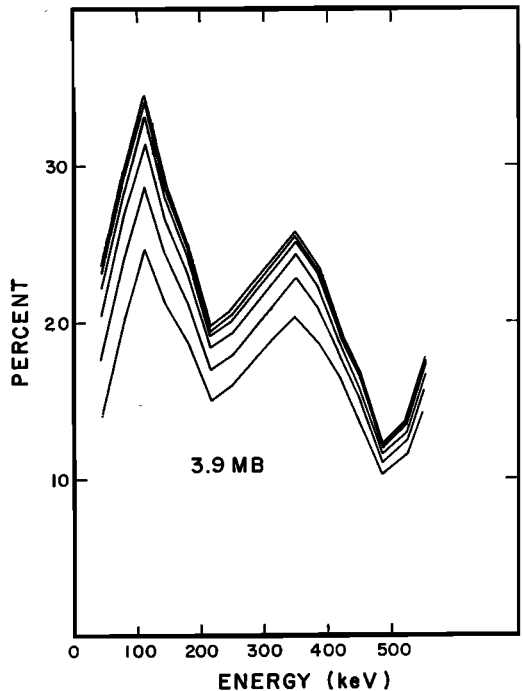

Fig. 12. Ratio of the intensity of the cosmic flux to the total flux measured at 3.9 mb over Texas, as a function of energy and zenith angle. The structure observed in the total spectrum is responsible for the complex shape of the curves. Zenith angle in 10° increments represents the parameter; 0° is the topmost curve.

from ~41.0° to ~43.5°N. The flux of gamma radiation observed at high balloon altitudes is strongly latitude dependent. It is seen that the latitude dependence is approximately like that previously found for the ionizing radiation at balloon altitudes [*Neher and Anderson*, 1962].

The centered-dipole geomagnetic latitude of Mildura is approximately 4° greater than that of Palestine. It is interesting and consistent with the above, that the balloon-altitude flux of photons with energies between 30 and 550 kev is about 30% more intense at Mildura than it is at Palestine. The increase is most apparent at low energies; the flux observed at energies greater than 100 kev is virtually the same at both locations.

The structure observed in the pulse-height spectrum at balloon altitudes has several causes. One such cause is the interaction of cosmic-ray neutrons with NaI. Slow neutron absorption by I^{127} produces gamma rays with energies up to 6.7 Mev; the levels of I^{128} are so closely spaced that a quasi-continuum results.

The high cross section for absorption of slow neutrons by I^{127}, coupled with the thickness of the collimator and the known flux of slow neutrons at these latitudes and altitudes, results in a negligible contribution by this component
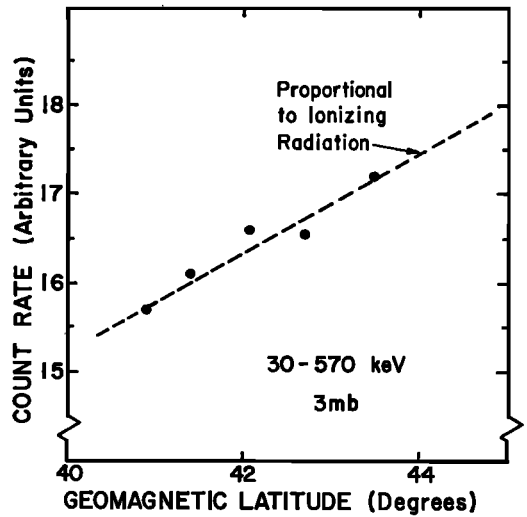

Fig. 14. Dependence of low-energy gamma radiation on geomagnetic latitude at ~3 g cm⁻² atmospheric depth. The count rates shown have been corrected for zenith angle effects.

of the secondary cosmic radiation to the counting rate of the central crystal.

Only fast neutrons that do not interact with the collimator may cause inelastic-scatter gamma radiation. The $(n, n'\ \gamma)$ excitations of I^{127} produce lines at 204 kev, 440 kev, and possibly at 490 kev.

If we use the total cross section for neutron absorption at neutron energies in excess of 100 kev [*Adair*, 1950], and assume that a neutron travels the average dimensions of the detector, an estimate may be made of the neutron transmission. The neutron transmission estimated in this manner for the collimator is ~10%.

Assuming 10% transmission of the solar-minimum neutron flux calculated for $\lambda \sim 40°$ by *Lingenfelter* [1963] and using the inelastic scatter cross section given by *Lind and Day* [1961], we find that the expected count rate at 0.204 Mev is approximately 0.3 c/s. This is in good agreement with the 0.31 c/s measured at that energy during 1967. The count rate calculated at 440 kev due to inelastic neutron scattering in sodium iodide also appears to be in agreement with the measurement.

The principal reason for the relatively large contribution by neutrons to the present experiment is the relatively large size of the central crystal and the fact that this crystal is well-
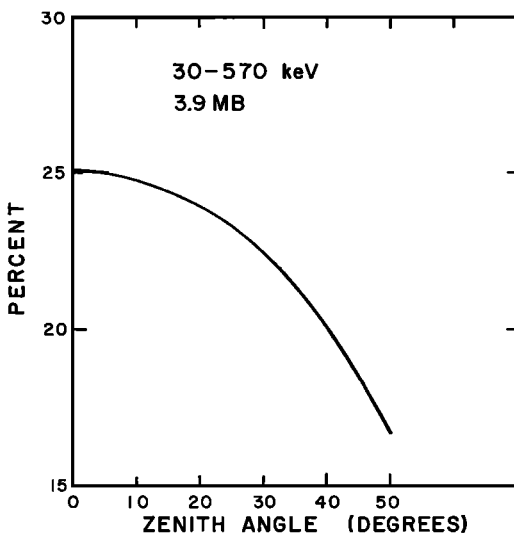

Fig. 13. Ratio of the intensity of the cosmic component to the total flux measured at 3.9 mb over Texas, as a function of zenith angle. A flat-earth approximation has been made.
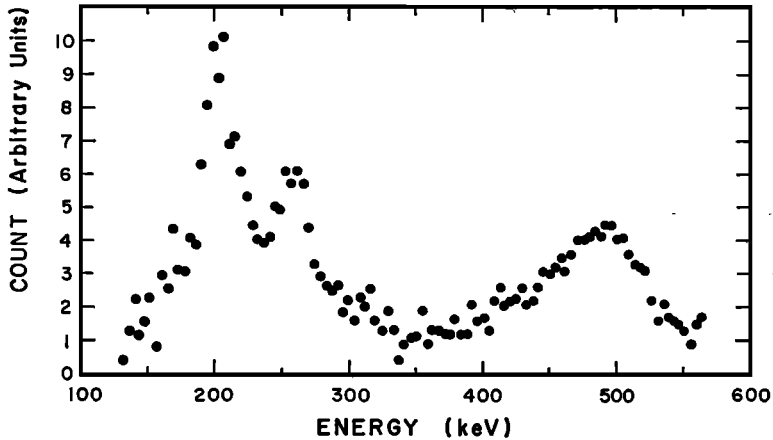
Fig. 15. Net spectrum recorded at high altitudes when an extrapolation of the power law detected at low energies is subtracted.

collimated for gamma radiation but not so for neutrons. Hence the neutron-to-gamma count rate ratio is larger in this experiment than it would be, say, in an experiment that employed a small phoswich.

The features observed in the spectrum at 260 and 490 kev remain unexplained. It is possible that the enhanced flux at 260 kev is the result of backscatter of high-energy photons, although the shape of this feature is like that produced by a line flux at that energy, rather than a backscatter peak. That it is probably not due to neutron effects is supported by the fact that no such line was observed when a Pu-Be neutron source was placed beside the detector in the laboratory.

A weak line has been observed by others at 490 kev [Shafroth, 1967] who were investigating neutron-NaI interactions, although we did not see it in our laboratory. A centroid-energy may be accurately assigned to the feature by fitting a Gaussian curve to it. The enhanced flux at 490 ± 5 kev (see Figure 15) is the most prominent feature above 400 kev in the spectrum measured at high balloon altitudes; it has exhibited the same degree of prominence and has occurred at the same energy at float altitudes on all of the flights we have conducted. While the energy resolution of the detector may be only ~65 kev at 0.5 Mev, the relatively large number of pulse-height analyzer channels used in the present experiment, together with the fact that the statistics

in each channel are reasonably good, permits a good determination of the profile of the feature to be made.

The presence of a 511-kev line has been reported by *Peterson* [1963] and by *Chupp et al.* [1967]. It is possible that they observed a feature similar to the one we have detected. Although it may be reasonable to assume a line at 511 kev, it has not been proven to exist. The apparatus used by *Peterson* [1963] had a limited number of pulse height channels; each had a width of approximately 40 kev, so that the energy analysis may not have been sufficiently detailed to differentiate between a peak at 490 kev and one at 511 kev. Inspection of the data presented by *Chupp et al.* [1967] indicated a feature at least 30 kev above 511 kev. Those authors also cited $Ru^{106} \rightarrow Rh^{106}$ decay from bomb debris that results in a 490-kev photon. In addition, they suggested the possibility of a 480-kev photon from the decay of cosmic-ray-produced Be^{7} in the atmosphere.

Considering the observed intensity at 511 kev, we may set an upper limit to the intensity of the annihilation radiation, by assuming that all of the counting rate at that energy is due to annihilation radiation. This figure is 0.45 ± 0.09 photon cm^{-2} sec^{-1}. The actual value of any 511-kev flux is probably much smaller than this, however, because of the contribution from the unresolved 490-kev feature and from the continuum. If a single-line assumption is made (even though the feature at 490 kev

appears too broad to be due to a single line) in the background spectrum, then the strength of that line is 0.5 ± 0.1 photon cm^{-2} sec^{-1}. The upper limit at the 95% confidence level for the flux of 511-kev radiation is 0.2 photon cm^{-2} sec^{-1}, at 3.9 mb and at midlatitudes. These fluxes may be compared with the 0.29 ± 0.04 photon cm^{-2} sec^{-1} reported by *Chupp et al.* [1967] over Texas. *Peterson* [1963] found 0.31 ± 0.03 count cm^{-2} sec^{-1} over Minnesota, for the strength of the feature near 0.5 Mev.

REFERENCES

Adair, R., Neutron cross sections of the elements, *Rev. Mod. Phys., 22,* 249, 1950.

Anderson, H., Ph.D. thesis, California Institute of Technology, Pasadena, California, 1961.

Anderson, H., L. Despain, and H. Neher, Response to environment and radiation of an ionization chamber and matched Geiger tube used on a spacecraft, *Nucl. Instr. Methods, 47,* 1, 1967.

Anderson, K., Cosmic ray photons below cascade energy, *Phys. Rev., 123,* 1435, 1961.

Axel, P., Intensity corrections for iodine X-rays escaping from sodium iodide scintillation crystals, *Rev. Sci. Instr., 25,* 391, 1954.

Bleeker, J., J. Burger, A. Deerenburg, A. Scheepmaker, B. Swanenburg, Y. Tanaka, S. Hayakawa, F. Makino, and H. Ogawa, Energy spectrum of diffuse primary X-rays up to 180 kev, *Can. J. Phys., 46,* 5461, 1968.

Brini, D., U. Ciregi, F. Fuligni, and E. Moretti, Low-energy cosmic-ray photons in atmosphere, *J. Geophys. Res., 72,* 903, 1967.

Chupp, E., A. Sarkady, and H. Gilman, The 0.5 Mev gamma ray flux and the energy loss spectrum in CsI(Tl) at 4 gm/cm², *Planetary Space Sci., 15,* 881, 1967.

Environmental Science Services Administration, *Solar-Geophysical Data,* Reports IER-FB-276' and IER-FB-277, 1967.

Environmental Science Services Administration, *Solar-Geophysical Data,* Reports IER-FB-285, and IER-FB-286, 1968.

Fazio, G., Gamma radiation from celestial objects, *Ann. Rev. Astron. Astrophys., 5,* 481, 1967.

Frost, K., E. Rothe, and L. Peterson, A search for the quiet-time solar gamma rays from balloon altitudes, *J. Geophys. Res., 71,* 4079, 1966.

Haymes, R., Fast neutrons in the earth's atmosphere, 1, Variation with depth, *J. Geophys. Res., 69,* 841, 1964.

Jones, F., Cosmic ray production of low-energy gamma rays, *J. Geophys. Res., 66,* 2029, 1961.

Lind, D., and R. Day, Studies of gamma rays from neutron inelastic scattering, *Ann. Phys., 12,* 485, 1961.

Lingenfelter, R., The cosmic-ray neutron leakage flux, *J. Geophys. Res., 68,* 5633, 1963.

Metzger, A., E. Anderson, M. Van Dilla, and J. Arnold, Detection of an interstellar flux of gamma-rays, *Nature, 204,* 766, 1964.

Miller, W., J. Reynolds, and W. Snow, Efficiencies and photofractions for sodium-iodide crystals, *Rev. Sci. Instr., 28,* 717, 1957.

Neher, H. V., An automatic ionization chamber, *Rev. Sci. Instr., 24,* 99, 1953.

Neher, H., and H. Anderson, Cosmic rays at balloon altitudes and the solar cycle, *J. Geophys. Res., 67,* 1309, 1962.

Neher, H., and A. Johnston, Modification to the automatic ionization chamber, *Rev. Sci. Instr., 27,* 173, 1956.

Neiler, J., and P. Bell, *Alpha-, Beta-, and Gamma-Ray Spectroscopy,* edited by K. Siegbahn, North-Holland Publishing Company, Amsterdam, 1965.

Perlow, G., and C. Kissinger, A search for primary cosmic gamma-radiation, 2, Low-energy radiation above and within the atmosphere, *Phys. Rev., 84,* 572, 1951.

Peterson, L., The 0.5 Mev gamma-ray and the low-energy gamma-ray spectrum to 6 grams per square centimeter over Minneapolis, *J. Geophys. Res., 68,* 979, 1963.

Puppi, G., and N. Dallaporta, The equilibrium of the cosmic ray beam in the atmosphere, *Progr. Cosmic Ray Phys., 1,* 315, 1952.

Shafroth, S., editor, *Scintillation Spectroscopy of Gamma Radiation,* vol. 1, Gordon and Breach, Inc., New York, 1967.

Vette, J., Low-energy gamma rays in air and in lead, *J. Geophys. Res., 67,* 1731, 1962.

Womack, E., and J. Overbeck, High resolution search for solar gamma-ray lines, *Bull. Am. Phys. Soc., 13,* 1398, 1968.